Pergamon

Int. J. Heat Mass Transfer. Vol. 37, No. 3, pp. 523–532, 1994

0017–9310/94 $6.00+0.00

When to defrost a refrigerator, and when to remove the scale from the heat exchanger of a power plant

ADRIAN BEJAN and JOSE V. C. VARGAS

Department of Mechanical Engineering and Materials Science, Box 90300, Duke University, Durham, NC 27708-0300, U.S.A.

and

JONG S. LIM

Samsung R&D Center, Refrigeration and Air-Con Lab, Consumer Electronics 416, Maetan-3 dong, Kwonsun-Gu, Suwon City, Kyungki-Do, Korea

(*Received* 16 *November* 1992 *and in final form* 15 *March* 1993)

Abstract—This paper demonstrates the existence of an optimal on/off sequence for operating a household refrigerator that accumulates ice on its evaporator coils. Experimentally it is shown that the rate of ice formation is constant in time. The optimal (intermittent) regime of operation determined in this paper minimizes the power required by the refrigerator, maintains the prescribed temperature of the cold space, and removes intermittently the ice layer. The second part of the paper proves that a similar strategy can be used for dealing with fouling in heat exchangers, i.e. for maximizing the power output of a power plant that is diminished by the formation of scale on its heat exchanger surfaces. These optimal on/off sequences of operation for refrigerators and power plants are proven based on pure heat transfer and thermodynamics grounds. The refrigerator and power plant models employed are the simplest models possible. Consequently, the optimal on/off sequences demonstrated in this paper are *fundamental* features that will be present (and deserve to be identified and exploited) in the design of actual refrigerators and power plants, no matter how complicated these designs may be.

1. INTRODUCTION

MOST OF us are familiar with the frosting and icing on the coils of household refrigerators, particularly when these operate in climates of high humidity. A layer of frost (ice and trapped air) builds up on the visible surface (e.g. bare or finned tubes) of the evaporator, which is surrounded by the cold air trapped in the cold space of the refrigerator. The growth of the ice layer leads to an increase in the thermal resistance between the cold space and the even colder evaporator surface. As this resistance increases, the temperature of the evaporator surface must decrease to continue to pull the appropriate refrigeration load out of the cold space. At the same time, the refrigerator works 'harder' as the compressor uses more electrical power to maintain the cold space at the prescribed temperature level.

Methods of coping with the formation of ice on the evaporator surface constitute a critical technology in the development of modern domestic refrigerators and freezers [1]. It is a technology that has stimulated considerable fundamental research on the formation of ice on tubes [2], and the melting of ice between fins [3, 4]. The most common de-icing method consists of interrupting the refrigeration cycle after a certain interval of operation, and then heating the evaporator (electrically, or by convection, or by reverse cycling) to melt the ice layer. In addition to this on/off sequence of operation, some designs call for the use of evaporator surfaces coated with water repelling substances, which prevent the stagnation of water droplets on the surface [5].

The conceptual work described in this paper was stimulated by the on/off sequence of operation that appears in the design of a modern defrosting refrigerator. Our first objective is to prove that there exists an *optimal* on/off sequence that minimizes the average power required by the refrigerator. We will demonstrate the existence of this optimum in a most fundamental way, i.e. based on purely heat transfer and thermodynamics grounds, and without recourse to economic considerations such as cost minimization.

Our second objective is to show that the optimal way of defrosting a refrigerator has an equally fundamental analog in power plant design. Fouling, or the buildup of scale on the heat exchanger surfaces located at the hot end and the cold end of the power cycle, has a detrimental effect on the efficiency of the cycle. In time, this effect becomes more pronounced and raises the question of what is the most appropriate moment to shut off the power cycle and clean the heat exchanger surfaces.

The similarity between the processes of heat

NOMENCLATURE

a	rate of ice buildup [m s^{-1}]
A	heat transfer area [m^2]
b	rate of scale buildup [m s^{-1}]
Bi	dimensionless group, equation (7)
Bi_*	dimensionless group, equation (23)
Bi_p	dimensionless group, equation (25)
C	the ratio q_J/q
F	dimensionless average power, equations (21), (24)
F_{max}	maximum dimensionless average power
h	heat transfer coefficient [W m^{-2} K^{-1}]
H	dimensionless group, equation (8)
k	thermal conductivity of ice or scale [W m^{-1} K^{-1}]
p	empirical constant, equation (16)
q	refrigerator heat leak [W]
q_J	Joule heating rate [W]
$\dot{Q}$	heat transfer rate [W]
t	time [s]
t_1	time when the cycle is on [s]
t_2	time when the cycle is off [s]
T_H	high temperature [K]
T_L	low temperature [K]
T_{max}	high temperature of working fluid [K]
T_{min}	low temperature of working fluid [K]
T_0	ambient temperature [K]
W	work [J]
$\dot{W}$	power [W].

Greek symbols

δ	thickness of ice or scale layer [m]
η_{II}	second law efficiency
θ	time ratio, equation (22)
τ	time ratio, equation (9).

Subscript

$(\,)_{opt}$	optimal.

exchanger fouling and evaporator icing has been recognized in the fouling heat transfer literature [6]. The challenge we faced in the second part of our paper was to demonstrate that the optimal on/off sequence of power plant operation can be based purely on heat transfer and thermodynamics arguments. It should be noted that economic cleaning schedules for process heat exchangers have been proposed in the heat exchanger literature [7–10]. These schedules, however, were based on economic arguments such as the minimization of the total cost that includes the cleaning cost and the power lost because of fouling [8]. The optimal operating regimes identified in this paper fall in the same class of fundamentals as the optimal time-dependent processes of energy storage and retrieval [11, 12].

2. REFRIGERATOR MODEL

Figure 1 shows the simplest features of a refrigerator (e.g. vapor compression cycle) that experiences icing on its evaporator (T_{min}). The function of the refrigerator modelled in Fig. 1 is to maintain the temperature of the refrigerated space (cold box) at a low level, T_L, in spite of the average heat transfer rate q that leaks steadily through the thermal insulation surrounding the cold space. The heat leak q reaches the cold box T_L, and is removed as $\dot{Q}$ during the time interval t_1 when the refrigerator is turned on,

$$\dot{Q} = \frac{q(t_1 + t_2)}{t_1}. \tag{1}$$

Each t_1 interval is followed by a time interval t_2 during which the refrigerator is turned off and the evaporator surface is being deiced. In this first treatment of the problem we assume that the defrosting time interval t_2 is known and fixed, and that the electric power used for melting the ice layer is negligible. The time interval in which the refrigerator must be left running, t_1, is the chief unknown of the problem. The refrigerator load $\dot{Q}$ is greater than the heat leak q,

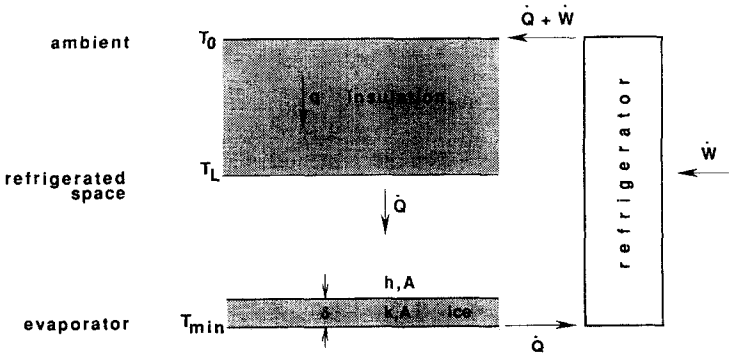

FIG. 1. Model of refrigerator with ice layer on the evaporator surface.

because the latter is being accumulated in the thermal inertia of the cold box during the time interval when the refrigeration cycle is turned off. We are assuming for simplicity that the cold box thermal inertia is large enough so that the temperature T_L is practically constant during each on/off cycle of total time length t_1+t_2. The refrigerator model is discussed further under equation (6).

The refrigeration cycle that operates between the ambient (T_0) and the inner evaporator surface (T_{min}) is irreversible, with a second law efficiency η_{II} assumed constant and known. The latter accounts for all the irreversibility features other than the finite temperature difference T_L-T_{min}, for example, the compressor isentropic efficiency less than one, the throttle, the pressure drops along the ducts, and the finite size of the room temperature condenser. These features are lumped into a constant η_{II} value between 0 and 1, because they are peripheral to the question posed in this problem and, as a good approximation, are insensitive to the formation of ice on the evaporator surface.

The feature that is affected by the formation of ice is the temperature gap T_L-T_{min}, which increases as the ice layer becomes thicker. The refrigeration load is driven into the evaporator by the temperature difference T_L-T_{min},

$$\dot{Q}=\left(\frac{1}{hA}+\frac{\delta}{kA}\right)^{-1}(T_L-T_{min}). \tag{2}$$

In this expression, A, h, δ and k are the evaporator surface, the convective heat transfer coefficient between the cooled material and the ice surface, the ice thickness, and the effective thermal conductivity of the frost layer (ice and trapped air). We further assume that A and h are constant, i.e. independent of δ.

3. EXPERIMENT TO DETERMINE $\delta(t)$

There is some disagreement on the way in which the thickness δ increases in time. Schneider's [13] measurements suggest a proportionality between δ and $t^{1/2}$, whereas Rite and Crawford's [2] experiments reveal a proportionality of the type $\delta \sim t$. Since the analytical form of the $\delta(t)$ function has a profound effect on the results of the optimization process, we performed our own experiment by using an instrumented household refrigerator positioned against the wall of an experimental chamber (Fig. 2). The two photographs inserted in the frame of the chamber show the interior (the instrumented refrigerator), and a view of the outside of the chamber, with the control and measurement instruments.

The chamber dimensions are 2.7×4.2 m in the plane of Fig. 2, and 3.67 m perpendicular to Fig. 2. The conditions inside the chamber were controlled carefully to simulate as realistically as possible the way in which an actual refrigerator is being used in a humid climate:

(a) The door of the cooling ('fridge') compartment was opened for 10 s once every 12 min.

(b) The door of the freezer compartment was opened for 10 s once every 40 min.

(c) The room temperature was 30°C.

(d) The relative humidity of the room air was 75%.

(e) The air temperatures in the cooling and freezer compartments were 3°C and −18°C, respectively.

These conditions are standard in the Korean refrigeration industry.

Photographs of the evaporator surface were taken at 40 min intervals, and the frost thickness was measured with a ruler on blow-ups of the photographs. The upper part of Fig. 3 shows the two photographs taken after $t=40$ and 440 min, during a run that started at 9:30 a.m. The insulation panel (foam) was partially removed, and replaced with a transparent film that was glued around the edges, to prevent the deposition of additional frost during photography. A ruler was aligned with the evaporator tube: the white arrowhead indicates the point on the plate fin on which the camera was focused. The thickness of the layer of frost (δ) formed on one side of the plate fin was measured on the blow-ups with an accuracy of 0.1 mm. The relative accuracy improved in time, as δ increased.

The $\delta(t)$ data collected during a 10 h run are shown in the lower part of Fig. 3. They were correlated very well by the straight line $\delta/t\cong0.42\ \text{mm h}^{-1}$. Our experiments validate Rite and Crawford's [2] conclusion that at the low air velocities and icing rates encountered in an actual refrigerator the icing rate is constant in time.

4. OPTIMAL ON/OFF SEQUENCE FOR REFRIGERATOR OPERATION

We assume therefore that the thickness of the ice layer increases as

$$\delta=at. \tag{3}$$

The rate of ice buildup, a, is assumed known from direct measurements. The power required by the refrigerator during the 'on' interval t_1 is

$$\dot{W}=\frac{1}{\eta_{II}}\dot{Q}\left(\frac{T_0}{T_{min}}-1\right) \tag{4}$$

for which $\dot{Q}$ is furnished by equation (2). The total work during the interval t_1 is

$$W=\int_0^{t_1}\dot{W}\,dt. \tag{5}$$

This work is used for the purpose of removing the corresponding heat leakage $\dot{Q}t_1$, or $q(t_1+t_2)$. It is worth mentioning that in a household refrigerator the compressor does not run continuously during the 'on'

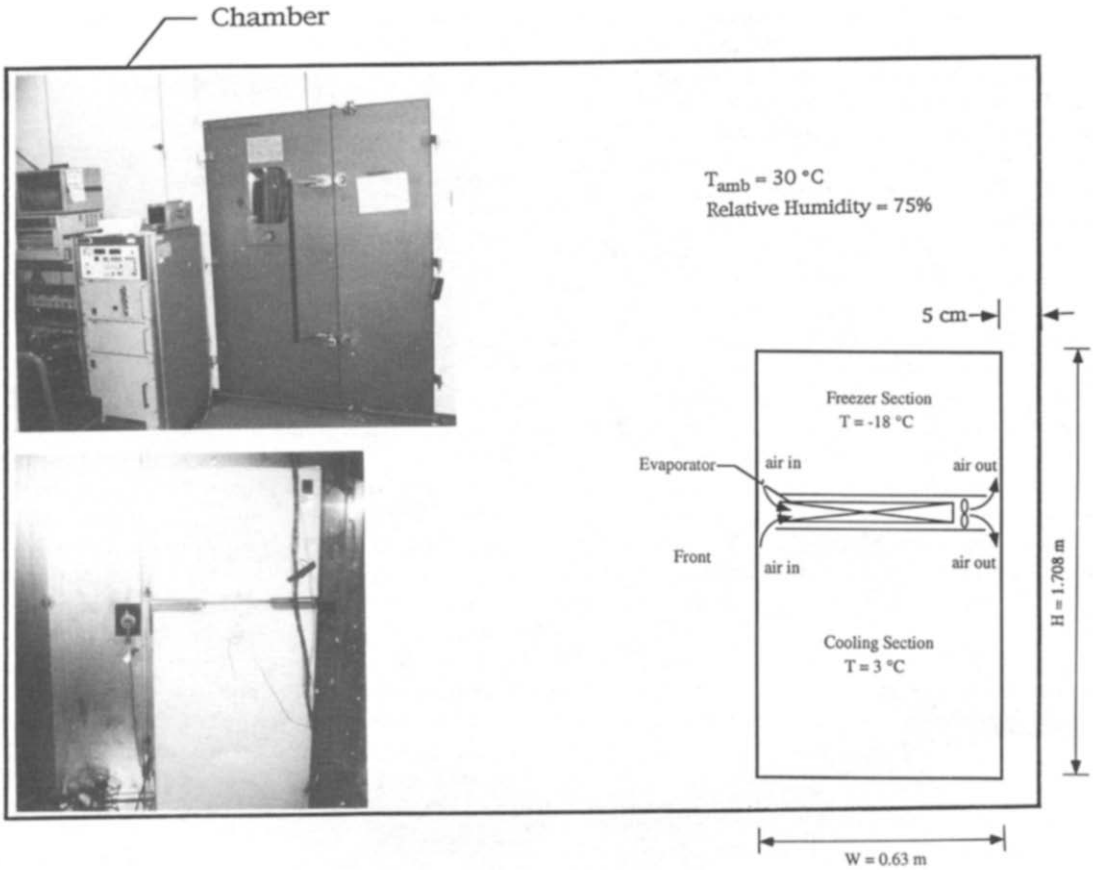

FIG. 2. The experimental chamber and the refrigerator used for measuring the rate of frost formation on the evaporator surface.

interval labeled t_1. The compressor runs intermittently (in short steps), typically 50% of the time. In other words, the instantaneous power $\dot{W}$ is the compressor power averaged over each pair of short steps. In conclusion, the figure of merit of the overall (macroscopic) on/off sequence of operation is the ratio $W/q(t_1+t_2)$. We show next that this ratio can be minimized by choosing an optimal time of refrigerator operation, t_1.

By combining equations (1)–(5) it is possible to express the average power requirement $W/(t_1+t_2)$ in the following nondimensional form,

$$\frac{\eta_{II} W}{q(t_1+t_2)} = \frac{(T_0/T_L)H}{Bi(1+\tau)} \times \ln\left[\frac{H-1-1/\tau}{H-1-(1/\tau)-Bi(1+\tau)}\right]-1 \quad (6)$$

where Bi is the Biot number based on the ice thickness of size at_2,

$$Bi = \frac{hat_2}{k} \quad (7)$$

and H is the nondimensional counterpart of the convective heat transfer coefficient,

$$H = \frac{hAT_L}{q}. \quad (8)$$

The Biot number may be viewed as a nondimensional rate of ice accumulation. In equations (6) and (8), T_L and T_0 are absolute temperatures. The nondimensional time τ is proportional to the time interval of refrigerator operation,

$$\tau = \frac{t_1}{t_2}. \quad (9)$$

Equation (6) shows that the work/heat ratio is a function of four dimensionless numbers, τ, H, Bi and T_0/T_L. Only τ represents a degree of freedom in the operation of the system, while the other three numbers are fixed as soon as the apparatus is constructed. In Fig. 4 we see that there exists an optimal time τ (or t_1) for minimum work/heat leak ratio, i.e. a best moment when the refrigeration should be interrupted for the purpose of deicing the evaporator. The upper drawing shows the shape of the energy demand curves when Bi is fixed, while the lower drawing shows the curves for constant H. The small time and large time asymptotes of all the curves shown in Fig. 4 are quite steep, and stress the importance of knowing the optimal τ value.

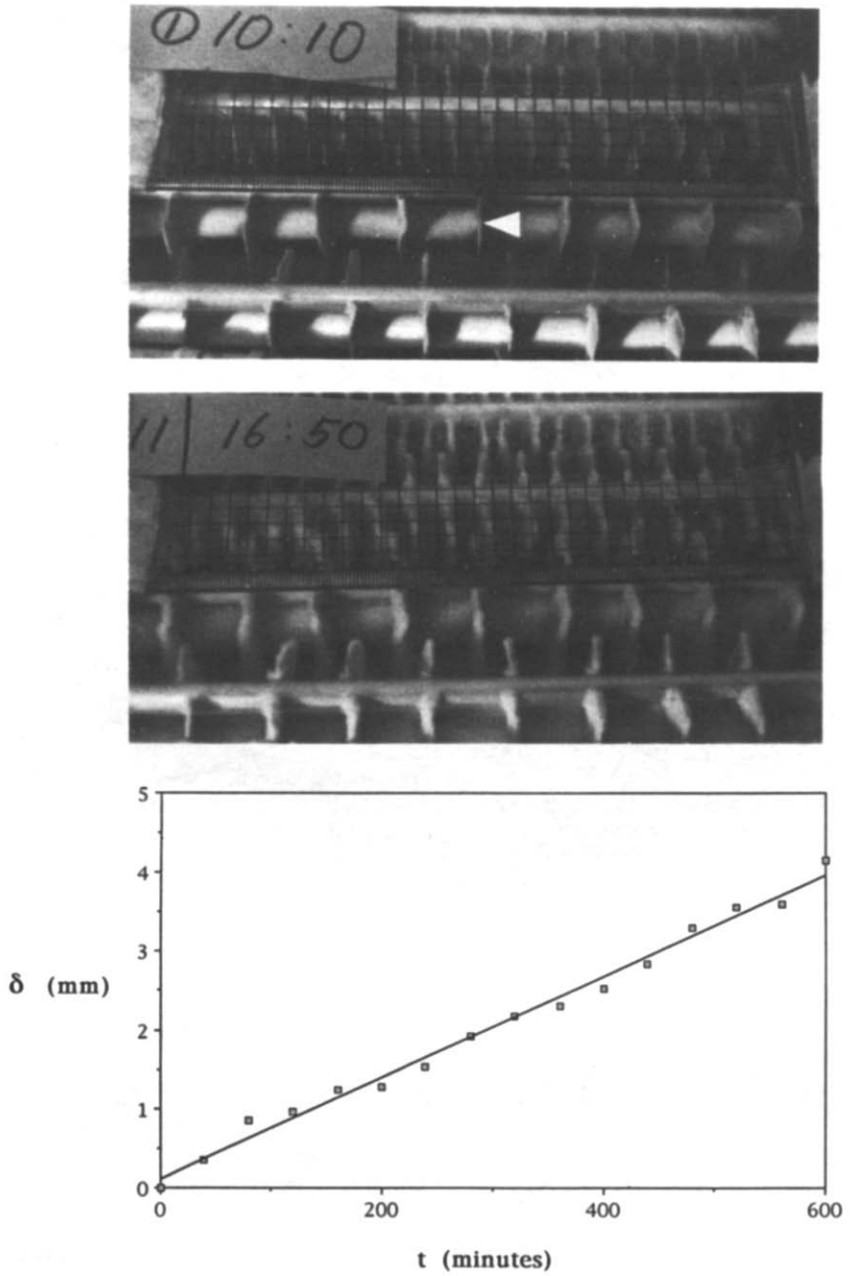

FIG. 3. Measurements showing the constant rate of frost formation on the evaporator of the experimental refrigerator (Fig. 2). The photographs show the evaporator surface during the experiment, at $t = 40$ min and, respectively, $t = 440$ min.

The optimal operating time is reported in Fig. 5. This was obtained numerically by minimizing the expression listed in equation (6). Unlike the right side of equation (6), which depends on four parameters including T_0/T_L, the optimal time τ_{opt} is a function of only two parameters, Bi and H. This can be seen also by taking the derivative $\partial/\partial\tau$ on the right side of equation (6) and setting it equal to zero. The upper drawing shows that when the group H is sufficiently large it has a negligible effect on τ_{opt}. The lower drawing shows that the optimal time of refrigerator operation is almost proportional to the inverse of Bi. The minimum work/heat leak ratio that corresponds to this optimal regime of operation can be calculated by substituting in equation (6) the $\tau_{opt}(Bi, H)$ value read off Fig. 5.

5. THE EFFECT OF THE ELECTRICAL POWER USED FOR MELTING THE ICE

Consider briefly what happens to the preceding conclusions if the electrical power used for resistively

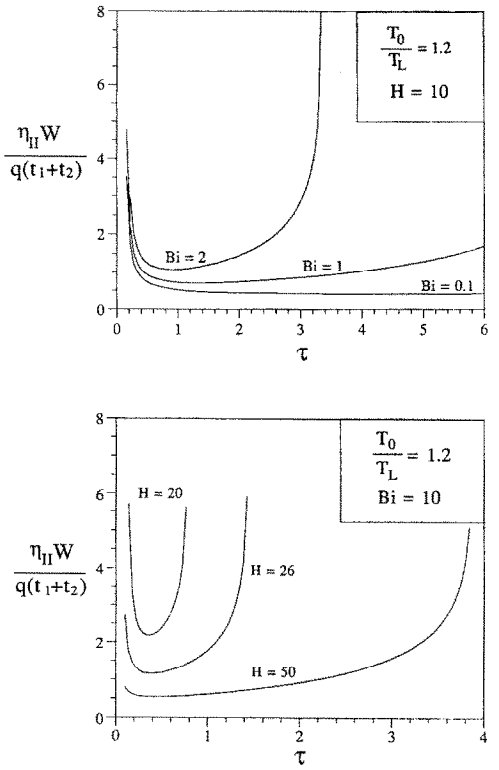

FIG. 4. Minimizing the work/heat leak ratio by choosing the optimal time interval for running the refrigerator (τ_* or t_1).

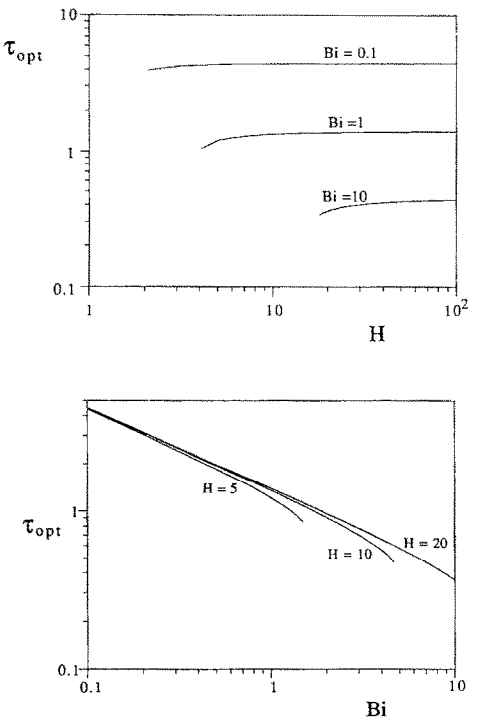

FIG. 5. The optimal time interval of refrigerator operation ($\delta = at$).

melting the ice is not negligible. If that power level (Joule heating rate) is the known constant q_J, equation (1) is replaced by

$$\dot{Q}t_1 = q(t_1+t_2)+q_Jt_2. \tag{10}$$

In place of equation (5), we write that the total work (electrical energy) that is required during the time t_1+t_2 is

$$W = \int_0^{t_1} \dot{W}\,dt+q_Jt_2. \tag{11}$$

If we make these changes, the analytical steps that gave us equation (6) lead this time to

$$\frac{\eta_{II}W}{q(t_1+t_2)} = \frac{(T_0/T_L)H}{Bi(1+\tau)} \times \ln\left[\frac{H-1-(1+C)/\tau}{H-1-Bi(1+\tau+C)-(1+C)/\tau}\right] -1-\frac{C(1-\eta_{II})}{1+\tau}. \tag{12}$$

The new constant C is shorthand for the ratio

$$C = \frac{q_J}{q} \tag{13}$$

and is assumed known. It is easy to see that equation (6) represents the $C\to 0$ limit of the more general equation (12).

The nondimensional average power requirement expressed by equation (12) was minimized numerically, and the results are presented in Fig. 6. The

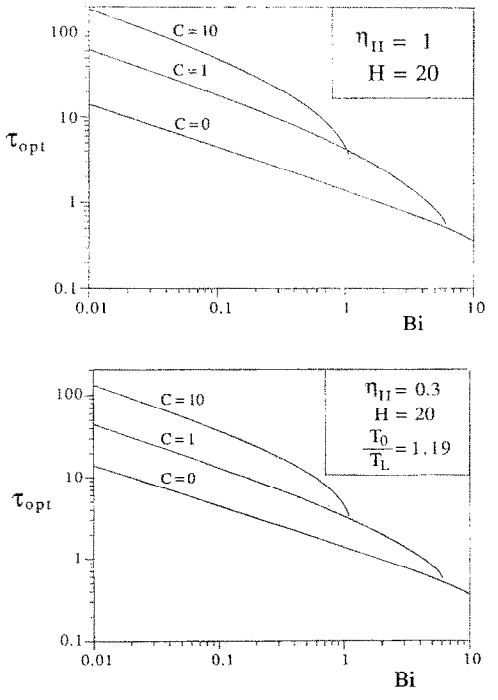

FIG. 6. The effect of electrical power used for melting the ice, q_J, on the optimal time interval of refrigerator operation ($\delta = at$).

optimal time of refrigerator operation ($\tau_{opt} = t_{1,opt}/t_2$) decreases with the Biot number, and increases as the C ratio increases. In the top frame of Fig. 6, where $\eta_{II} = 1$, τ_{opt} depends only on Bi, H and C. As shown in the lower frame and equation (12), when $\eta_{II} < 1$ the optimal time τ_{opt} depends on η_{II} and T_0/T_L, in addition to Bi, H and C. The lower graph was drawn for $\eta_{II} = 0.3$, $T_0 = 30°C$ and $T_L = -18°C$, which means $T_0/T_L = 1.19$. Taken together, the two graphs of Fig. 6 show that η_{II} and T_0/T_L have only a minor effect on τ_{opt} when C is smaller than 1.

Numerical example. We will show how the present results (Fig. 6) can be used to calculate the optimal time when to shut off the refrigeration cycle and start the defrosting of the evaporator. The representative data for a domestic refrigerator such as the one used in the experiment are: $q = 60$ W, $q_J = 100$ W, $h = 40$ W m^{-2} K^{-1}, $t_2 = 0.5$ h, $T_L = -18°C$, $A = 0.1$ m^2, and $a = 0.42$ mm h^{-1}. The representative thermal conductivity of fresh frost is roughly $k \cong 0.2$ W m^{-1} K^{-1} (Yonko and Sepsy [14]). With these values we calculate $C = 1.67$, $Bi \cong 0.04$ and $H \cong 34$. Since H does not have a significant effect when Bi is small (see Fig. 5, bottom), we may use the lower frame of Fig. 6 for $Bi = 0.04$ and $C = 1.67$, and read approximately $\tau_{opt} \cong 24$. The optimal time of refrigerator operation is therefore $t_{1,opt} = \tau_{opt} t_2 \cong 12$ h.

6. POWER PLANT WITH SCALE ON THE HOT-END HEAT EXCHANGER SURFACE

We now turn our attention to a related fundamental problem that occurs in the operation of a power plant in which the working fluid fouls gradually (i.e. deposits scale on) the heat exchanger surfaces. The scale adds to the overall thermal resistance of the heat exchanger, and induces a steady decrease in the energy conversion efficiency of the power plant. The question is when to shut off the power plant for the purpose of removing the scale from the heat exchanger surfaces.

In Fig. 7 we see what perhaps is the simplest model in which we can examine this fundamental engineering question. The heat source (e.g. flame) temperature level T_H is fixed, while the working fluid (e.g. water) executes a cycle between the high temperature T_{max} and the ambient T_0. The heat exchanger that, in time, experiences fouling is assumed to be located at the hot end of the cycle, in the temperature gap $T_H - T_{max}$. The thermal resistance of this heat exchanger is due to its finite heat transfer area A, the finite heat transfer coefficient h between the heat source and the surface of the scale, and the scale itself.

We assume that the scale thickness δ varies (increases) with the time of operation, $\delta = f(t)$. The rate of heat transfer that drives the power cycle is

$$\dot{Q} = \left(\frac{1}{hA} + \frac{\delta}{kA}\right)^{-1} (T_H - T_{max}). \tag{14}$$

For the sake of brevity and clarity we begin with the linear model

$$\delta = bt \tag{15}$$

in which the fouling rate b is assumed to be a known empirical constant. Later, we will report the results based on the more general exponential growth model proposed by Kern and Seaton [15],

$$\delta = p\left[1 - \exp\left(-\frac{b}{p}t\right)\right] \tag{16}$$

which reduces to equation (15) as $p \to \infty$. The Kern and Seaton model relies on two empirical constants, the initial growth rate b, and the long-time ('plateau') thickness p. Epstein's [6] review and, more recently, the experiments described by Konings [16] show that the experimentally measured thickness can be fitted with equation (16) and, at small times, with equation (15).

7. OPTIMAL ON/OFF SEQUENCE FOR MAXIMUM AVERAGE POWER

Let t_1 be the unknown time interval in which the power plant is on, and t_2 the known and fixed cleaning time interval that follows t_1. The power plant is shut down during t_2. If we are interested in producing

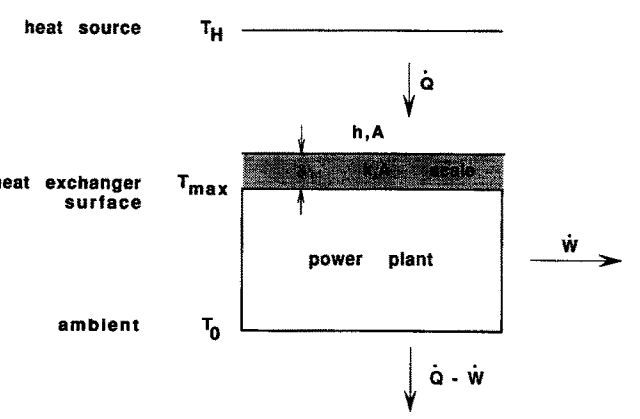

FIG. 7. Model of power plant with scale on the hot-end heat exchanger surface.

maximum power averaged over time, we must maximize the ratio $W/(t_1+t_2)$, where W is the work produced while the power plant is on,

$$W = \int_0^{t_1} \dot{W}\,dt. \tag{17}$$

In this problem there are two parameters, t_1 and T_{max}, that can be chosen optimally such that the average power output $W/(t_1+t_2)$ is maximized. The selection of the optimal T_{max} is now a classical result derived independently by Novikov [17] (see also El-Wakil [18]) and Curzon and Ahlborn [19] (see also Bejan [20]). For example, if the power cycle executed between T_{max} and T_0 is reversible, the instantaneous power output $\dot{W}$ is maximum if T_{max} has the *constant* value

$$T_{max,opt} = (T_H T_0)^{1/2}. \tag{18}$$

If the expansion through the turbine is irreversible, the expression for $T_{max,opt}$ is somewhat more complicated (Novikov [17]), but it is still a constant (it depends on T_0, T_H, and the turbine characteristics). The fact that $T_{max,opt}$ is constant and independent of t_1 is an important feature that must be kept in mind as we turn our attention to the optimal selection of the second free parameter, t_1.

The instantaneous power output maximized with respect to T_{max} is

$$\dot{W} = \eta_{II}\left(1 - \frac{T_0}{T_{max,opt}}\right)\dot{Q} \tag{19}$$

where the second law efficiency constant η_{II} accounts for the assumed irreversibility of the power cycle, and where $T_{max,opt}$ is a constant depending on T_0, T_H and η_{II}.

Linear $\delta(t)$ model. By combining the linear model (15) with equations (14), (17) and (19) it can be shown that the time averaged power output is given by the expression

$$\frac{W}{t_1+t_2} = \eta_{II}\left(1 - \frac{T_0}{T_{max,opt}}\right)(T_H - T_{max,opt})hA \cdot F(\theta, Bi_*) \tag{20}$$

where

$$F(\theta, Bi_*) = \frac{\ln(1+\theta Bi_*)}{(1+\theta)Bi_*} \tag{21}$$

$$\theta = \frac{t_1}{t_2} \tag{22}$$

$$Bi_* = \frac{hbt_2}{k}. \tag{23}$$

Noteworthy in these definitions are the nondimensional time interval of power plant operation, θ, and the nondimensional ratio of fouling, Bi_*. The effect of θ and Bi_* on the average power output is conveyed by the function $F(\theta, Bi_*)$ which is shown plotted in Fig. 8. The average power output reaches a maximum at a distinct operating time, θ_{opt}.

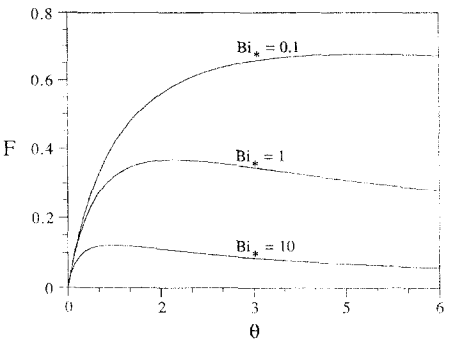

FIG. 8. The effect of time of operation and rate of fouling on the average power output; linear $\delta(t)$ model.

Figure 9 shows how the group Bi_* influences the optimal operating time and the corresponding maximum average power. The Bi_* number may be seen as a way of nondimensionalizing the known cleaning time t_2. The figure shows that as the cleaning time decreases the maximum average power and the time ratio θ_{opt} increases. The optimal time interval of power plant operation, $t_{1,opt}$, is proportional to the group $\theta_{opt} \cdot Bi_*$: the dash line in Fig. 9 shows that this time interval decreases as the cleaning time decreases. The ratio θ_{opt} indicates that $t_{1,opt}$ does not decrease as fast as t_2 when t_2 decreases.

Exponential $\delta(t)$ model. If in the preceding analysis the linear model (15) is replaced with the exponential $\delta(t)$ model (16), the expression for the average power output continues to be represented by equation (20) with the following definitions

$$F(\theta, Bi_*, Bi_p) = \frac{\theta Bi_* + Bi_p \ln[1 + Bi_p - Bi_p \exp(-Bi_*\theta/Bi_p)]}{(1+\theta)Bi_*(1+Bi_p)} \tag{24}$$

$$Bi_p = \frac{hp}{k}. \tag{25}$$

The new dimensionless number Bi_p is the Biot number based on the long-time thickness of the scale, p. It is easy to show that equation (24) reduces to equation (21) as $Bi_p \to \infty$.

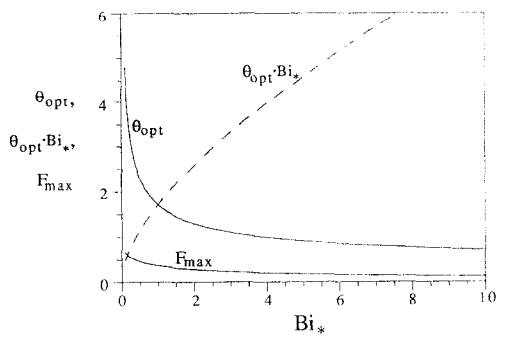

FIG. 9. The optimal time interval of power plant operation, and the maximum average power output; linear $\delta(t)$ model.

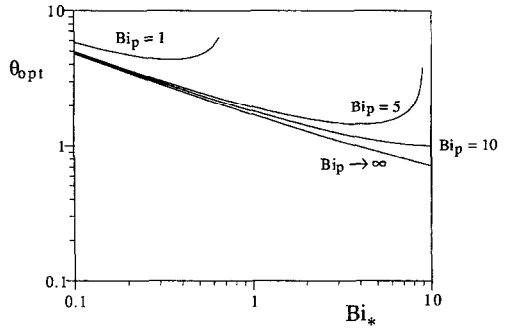

FIG. 10. The effect of the Bi_p number on the optimal time ratio; exponential $\delta(t)$ model.

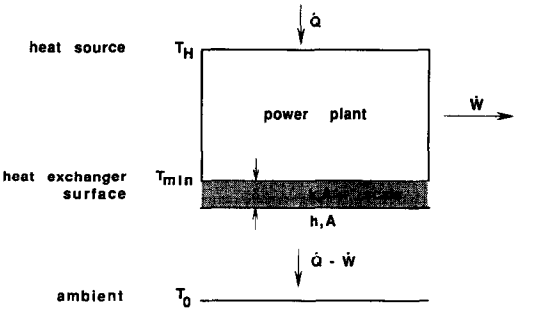

FIG. 12. Model of power plant with scale on the cold-end heat exchanger surface.

The numerical maximization of F leads to the two-parameter charts shown in Figs. 10 and 11. The two parameters, Bi_* and Bi_p, account for the two empirical constants that were used to curvefit $\delta(t)$ in accordance with equation (16). Figure 10 shows that when $Bi_p \lesssim 10$, this new parameter has a significant effect on the optimal time ratio θ_{opt}: specifically, θ_{opt} increases noticeably as Bi_p decreases. The same parameter has a less pronounced effect on the maximum average power F_{max}, which is plotted in Fig. 11.

8. POWER PLANT WITH SCALE ON THE COLD-END HEAT EXCHANGER SURFACE

Consider now a power plant in which fouling occurs at the cold end of the cycle, for example, on the condenser. We will show that the nondimensional results obtained in Figs. 9–11 for power plants with fouling at the hot end apply unchanged when fouling occurs at the cold end.

Figure 12 shows a simple model for a power plant with scale on the cold-end heat exchanger surface. Repeated in this model are all the features that were encountered first in Fig. 7. The power cycle contained between T_H and T_{min} is not necessarily reversible, and its second law efficiency is η_{II}. In time, the scale of thickness $\delta(t)$ augments the thermal resistance between the working fluid (T_{min}) and the ambient (T_0):

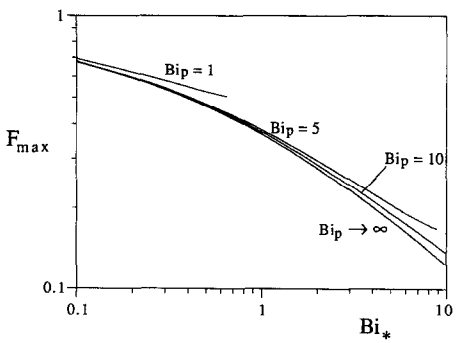

FIG. 11. The effect of the Bi_p number on the maximum average power; exponential $\delta(t)$ model.

$$\dot{Q} - \dot{W} = \left(\frac{1}{hA} + \frac{\delta}{kA}\right)^{-1} (T_{min} - T_0). \tag{26}$$

For the reasons discussed above and below equation (18) in the preceding section, the instantaneous power output $\dot{W}$ can be optimized first with respect to T_{min}. The resulting optimal temperature $T_{min,opt}$ is a function of T_H, T_0 and η_{II}, for example, $T_{min,opt} = (T_H T_0)^{1/2}$ if $\eta_{II} = 1$. Because of this result, in the following analysis we assume that $T_{min,opt}$ is known, and use $T_{min} = T_{min,opt}$. The instantaneous power maximized in this manner is

$$\dot{W} = \eta_{II}\left(1 - \frac{T_{min,opt}}{T_H}\right)\dot{Q}. \tag{27}$$

The power plant operates during the time interval t_1, and the fouled surface is cleaned during the following interval of length t_2. The analysis consists of two steps. First, the total work W produced during the interval t_1 is calculated with equation (17), by using equations (26), (27) and an appropriate model of $\delta(t)$. Second, the average power is calculated as $W/(t_1+t_2)$. For brevity we show only the final result,

$$\frac{W}{t_1+t_2} = \frac{\eta_{II}(1 - T_{min,opt}/T_H)}{1 - \eta_{II}(1 - T_{min,opt}/T_H)} \times (T_{min,opt} - T_0)hA \cdot F(\theta, Bi_*, Bi_p) \tag{28}$$

in which the function F has the same form as in equations (21) and (24), depending on whether we use the linear model or the exponential model for $\delta(t)$. This means that the maximization of the average power with respect to the interval of operation, θ, leads to exactly the same curves as the ones seen in Figs. 9–11.

In conclusion, the *nondimensional* results of Figs. 9–11 are general, in the sense that the fouled heat exchanger may be located either at the hot end or at the cold end of the cycle executed by the working fluid. The physical (i.e. dimensional) results, however, differ from one case to the other. In this section, the groups Bi_* and Bi_p are based on properties of the cold-end heat exchanger (h, k, b, p), in accordance with the model of Fig. 12.

9. CONCLUDING REMARKS

In this paper we used the most fundamental principles of heat transfer and thermodynamics to demonstrate the existence of an optimal on/off sequence for refrigerator operation, which (1) minimizes the average consumption of electrical power, (2) maintains the prescribed low temperature in the cold space, and (3) removes intermittently the ice layer that accumulates on the evaporator surface. We demonstrated this by using the simplest possible refrigerator model. This means that the optimal on/off sequence is a fundamental feature that must be identified (and exploited) in the design of any type of defrosting refrigerator, no matter how complicated that design may be.

In the second part of the paper, we relied once again on the most fundamental principles of heat transfer and thermodynamics to prove that an optimal on/off sequence exists in power plant design. Intervals of power plant operation must be interspaced optimally with intervals for the removal of scale from heat exchanger surfaces so that, in time, the average power output of the plant is maximum. The power plant model used in this demonstration was the simplest. An optimal on/off sequence of the type described in this paper will be present in the design of any power plant that experiences fouling, regardless of the complexity of the design, or whether fouling occurs at the hot end of the cycle or at the cold end.

REFERENCES

1. T. J. Dossat, *Principles of Refrigeration* (2nd Edn), Chaps. 11 and 20. Wiley, New York (1981).
2. R. W. Rite and R. R. Crawford, An experimental investigation of air-side heat and mass transfer on domestic refrigerator-freezer finned-tube evaporators. *Proc. XVIIIth Int. Congress of Ref.*, Montreal, Quebec, Canada, pp. 806–810, 10–17 August (1991).
3. S. Nagakubo and A. Saito, Numerical analysis of direct contact melting process, *Trans. Jap. Assoc. Refrigeration* **4**(3), 37–45 (1987) (in Japanese).
4. A. Saito, T. Imamura, Y. Utaka and A. Saito, On the contact heat transfer with melting (direct contact melting process within an inclined rectangular cross-section). *JSME Int. J., Series II* **32**(3), 411–419 (1989).
5. Y. Tsuda and A. Iwamoto, Antifrosting heat exchanger. *National Technical Report* **38**, 108–113 (1992) (in Japanese).
6. N. Epstein, Fouling in heat exchangers. *Heat Transfer 1978—Proc. 6th Int. Heat Transfer Conf.*, Vol. 6, pp. 235–253. Hemisphere, New York (1979).
7. E. F. C. Somerscales, Fouling of heat transfer surfaces: an historical review, *Heat Transfer Engng* **11**(1), 19–36 (1990).
8. C. E. Colborn, Determining the economical interval between cleanings of condenser tubes, *Power* **58**, 803–805 (1923).
9. W. L. Badger and D. F. Othmer, Studies in evaporator design—VIII. Optimum cycle for liquids which form scale, *Trans. AIChE* **16**(2), 159–168 (1924).
10. W. L. McCabe, Economic side of evaporator scale formation, *Chem. Metall. Engng* **33**(2), 86–87 (1926).
11. A. Bejan, Two thermodynamic optima in the design of sensible heat units for energy storage, *J. Heat Transfer* **100**, 708–712 (1978).
12. R. J. Krane, A second law analysis of the optimum design and operation of thermal energy systems, *Int. J. Heat Mass Transfer* **30**, 43–57 (1987).
13. H. W. Schneider, Equation of the growth rate of frost forming on cooled surfaces, *Int. J. Heat Mass Transfer* **21**, 1019–1024 (1978).
14. J. D. Yonko and C. F. Sepsy, An investigation of the thermal conductivity of frost while forming on a flat horizontal plate, Paper No. 2043, *ASHRAE 74th Annual Meeting*, Minneapolis (1967).
15. D. Q. Kern and R. E. Seaton, Surface fouling: how to calculate limits, *Chem. Engng Prog.* **55**(6), 71–73 (1959).
16. A. M. Konings, Guide values for the fouling resistances of cooling water with different types of treatment for design of shell-and-tube heat exchangers, *Heat Transfer Engng* **10**, 54–61 (1989).
17. I. I. Novikov, The efficiency of atomic power stations, *J. Nuclear Energy II* **7**, 125–128 (1958); translated from *Atomnaya Energiya* **3**(11), 409 (1957).
18. M. M. El-Wakil, *Nuclear Power Engineering*, pp. 162–165. McGraw-Hill, New York (1962).
19. F. L. Curzon and B. Ahlborn, Efficiency of a Carnot engine at maximum power output, *Am. J. Phys.* **43**, 22–24 (1975).
20. A. Bejan, *Advanced Engineering Thermodynamics*, Chap. 8. Wiley, New York (1988).